An introduction to Orthogonal Time Frequency Space (OTFS) modulation for high mobility communications

Emanuele Viterbo

Department of Electrical and Computer Systems Engineering
Monash University, Clayton, Australia

November, 2019

Special thanks to P. Raviteja and Yi Hong

Overview I

1. Introduction
   - Evolution of wireless
   - High-Doppler wireless channels
   - Conventional modulation scheme – OFDM
   - Effect of high Dopplers in conventional modulation
2. Wireless channel representation
   - Time–frequency representation
   - Time–delay representation
   - Delay–Doppler representation
3. OTFS modulation
   - Signaling in the delay–Doppler domain

Overview II

4. OTFS Input-Output Relation in Matrix Form

5. OTFS Signal Detection
   - Vectorized formulation of the input-output relation
   - Message passing based detection

Introduction

Evolution of wireless

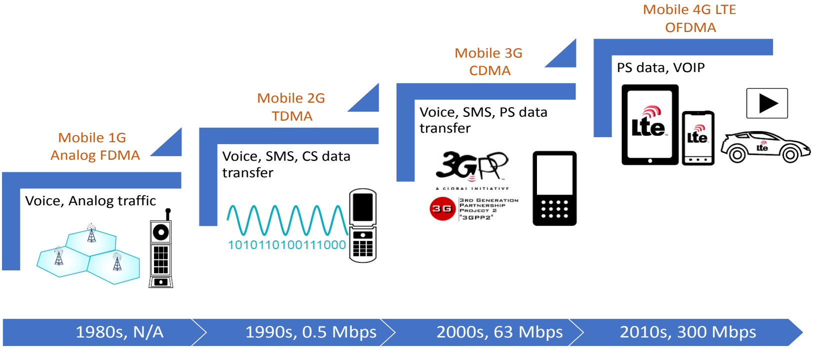

- Waveform design is the major change between the generations

High-Doppler wireless channels

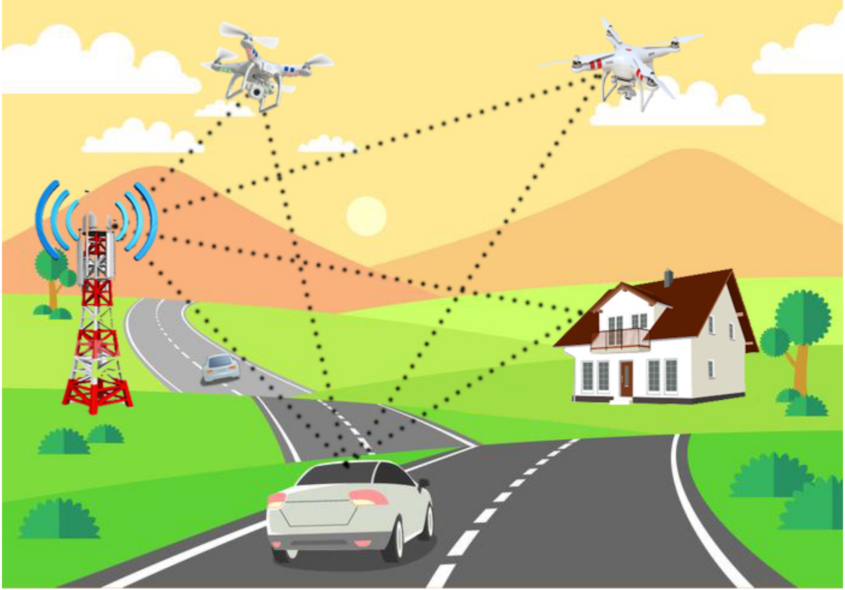

Wireless Channels - delay spread

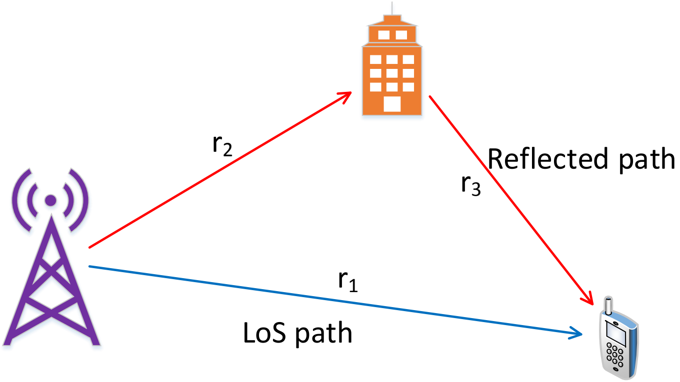

- Delay of LoS path: $\tau_1 = r_1/c$
- Delay of reflected path: $\tau_2 = (r_2 + r_3)/c$
- Delay spread: $\tau_2 - \tau_1$

Wireless Channels - Doppler spread

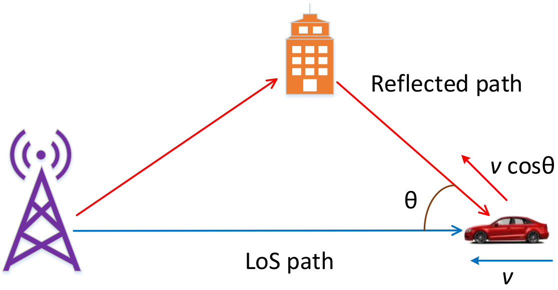

- Doppler frequency of LoS path: $\nu_1 = f_c \frac{v}{c}$
- Doppler frequency of reflected path: $\nu_2 = f_c \frac{v \cos\theta}{c}$
- Doppler spread: $\nu_2 - \nu_1$

TX: $s(t)$ **RX:** $r(t) = h_1 s(t - \tau_1) e^{-j2\pi\nu_1 t} + h_2 s(t - \tau_2) e^{-j2\pi\nu_2 t}$

Typical delay and Doppler spreads

Delay spread ($c = 3 \cdot 10^8$m/s)

Δr_{max}	Indoor (3m)	Outdoor (3km)
τ_{max}	10ns	10μs

Doppler spread

ν_{max}	$f_c = $ 2GHz	$f_c = $ 60GHz
$v = 1.5$m/s $= 5.5$km/h	10Hz	300Hz
$v = 3$m/s $= 11$km/h	20Hz	600Hz
$v = 30$m/s $= 110$km/h	200Hz	6KHz
$v = 150$m/s $= 550$km/h	1KHz	30KHz

Conventional modulation scheme – OFDM

- OFDM - Orthogonal Frequency Division Multiplexing

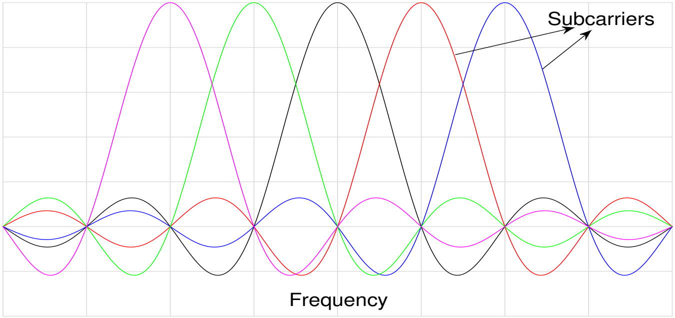

- OFDM divides the frequency selective channel into M parallel sub-channels

OFDM system model

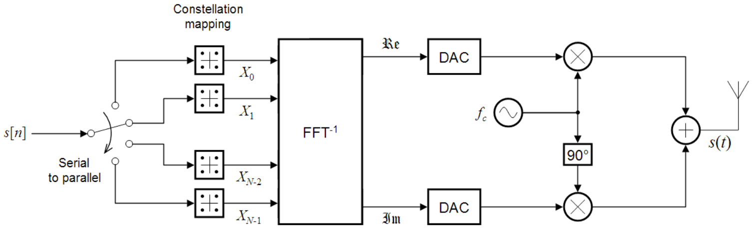

Figure: OFDM Tx

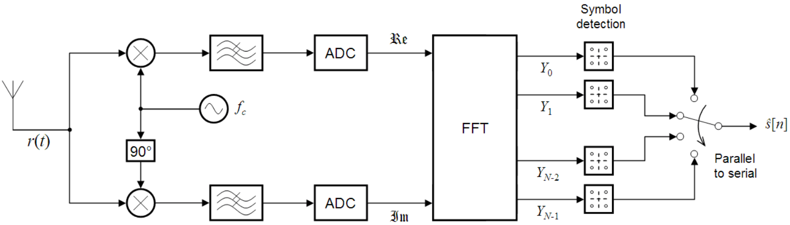

Figure: OFDM Rx

(*) From Wikipedia, the free encyclopedia

OFDM system model

- Received signal – channel is constant over OFDM symbol (no Doppler)
  $\mathbf{h} = (h_0, h_1, \cdots, h_{P-1})$ – Path gains over P taps

$$\mathbf{r} = \mathbf{h} \circledast \mathbf{s} = \underbrace{\begin{bmatrix} h_0 & 0 & \cdots & 0 & h_{P-1} & h_{P-2} & \cdots & h_1 \\ h_1 & h_0 & \cdots & 0 & 0 & h_{P-1} & \cdots & h_2 \\ \vdots & \ddots & \ddots & \ddots & \ddots & \ddots & \ddots & \vdots \\ \vdots & \ddots & \ddots & \ddots & \ddots & \ddots & \ddots & h_{P-1} \\ h_{P-1} & \ddots & \ddots & \ddots & \ddots & \ddots & \ddots & \vdots \\ \vdots & \ddots & \ddots & \ddots & \ddots & \ddots & \ddots & \vdots \\ \vdots & \ddots & \ddots & \ddots & \ddots & \ddots & \ddots & \vdots \\ 0 & 0 & \cdots & h_{P-1} & h_{P-2} & \cdots & h_1 & h_0 \end{bmatrix}}_{M \times M \text{ Circulant matrix } (\mathbf{H})} \mathbf{s}$$

- Eigenvalue decomposition property $\mathbf{H} = \mathbf{F}^H \mathbf{D} \mathbf{F}$ where $\mathbf{D} = \text{diag}[DFT_M(\mathbf{h})]$

OFDM system model

- At the receiver we have

$$\mathbf{r} = \mathbf{F}^H \mathbf{D} \mathbf{F} \mathbf{s} = \sum_{i=0}^{P-1} h_i \mathbf{\Pi}^i \mathbf{s}$$

where $\mathbf{\Pi}$ is the permutation matrix $\begin{pmatrix} 0 & \cdots & 0 & 1 \\ 1 & \ddots & 0 & 0 \\ \vdots & \ddots & \ddots & \vdots \\ 0 & \cdots & 1 & 0 \end{pmatrix}$

(notation used later as alternative representation of the channel)

- At the receiver we have input-output relation in frequency domain

$$\mathbf{y} = \mathbf{F}\mathbf{r} = \underbrace{\mathbf{D}}_{\text{Diagonal matrix with subcarrier gains}} \mathbf{x}$$

- OFDM Pros
  - Simple detection (one tap equalizer)
  - Efficiently combat the multi-path effects

Effect of high multiple Dopplers in OFDM

- **H** matrix lost the circulant structure – decomposition becomes erroneous
- Introduces inter carrier interference (ICI)

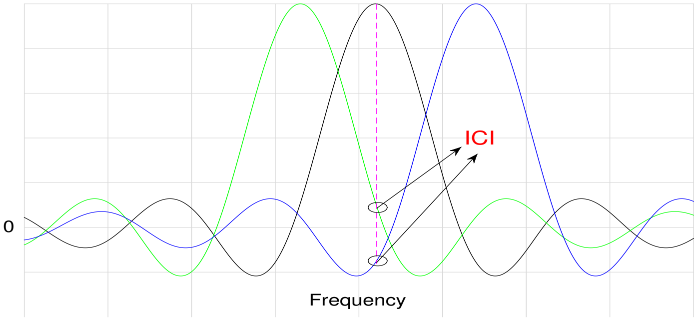

- OFDM Cons
  - multiple Dopplers are difficult to equalize
  - Sub-channel gains are not equal and lowest gain decides the performance

Effect of high Dopplers in OFDM

- Orthogonal Time Frequency Space Modulation (OTFS)$^{(*)}$
  - Solves the two cons of OFDM
  - Works in Delay–Doppler domain rather than Time–Frequency domain

(*) R. Hadani, S. Rakib, M. Tsatsanis, A. Monk, A. J. Goldsmith, A. F. Molisch, and R. Calderbank, "Orthogonal time frequency space modulation," in *Proc. IEEE WCNC*, San Francisco, CA, USA, March 2017.

cohere technologies

Wireless channel representation

Wireless channel representation

- Different representations of linear time variant (LTV) wireless channels

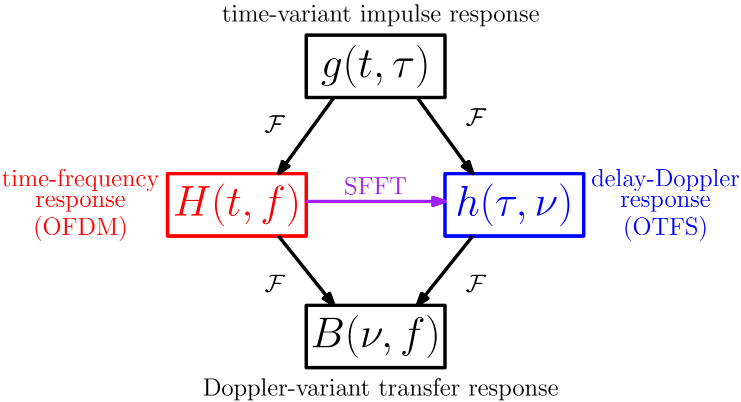

Wireless channel representation

- The received signal in linear time variant channel (LTV)

$$r(t) = \int \underbrace{g(t,\tau)}_{\text{time-variant impulse response}} s(t-\tau)d\tau \rightarrow \text{generalization of LTI}$$

$$= \int\int \underbrace{h(\tau,\nu)}_{\text{Delay–Doppler spreading function}} s(t-\tau)e^{j2\pi\nu t}d\tau d\nu \rightarrow \text{Delay–Doppler Channel}$$

$$= \int \underbrace{H(t,f)}_{\text{time-frequency response}} S(f)e^{j2\pi ft}df \rightarrow \text{Time–Frequency Channel}$$

- Relation between $h(\tau,\nu)$ and $H(t,f)$

$$\left.\begin{aligned} h(\tau,\nu) &= \int\int H(t,f)e^{-j2\pi(\nu t - f\tau)}dtdf \\ H(t,f) &= \int\int h(\tau,\nu)e^{j2\pi(\nu t - f\tau)}d\tau d\nu \end{aligned}\right\}\text{Pair of 2D symplectic FT}$$

Wireless channel representation

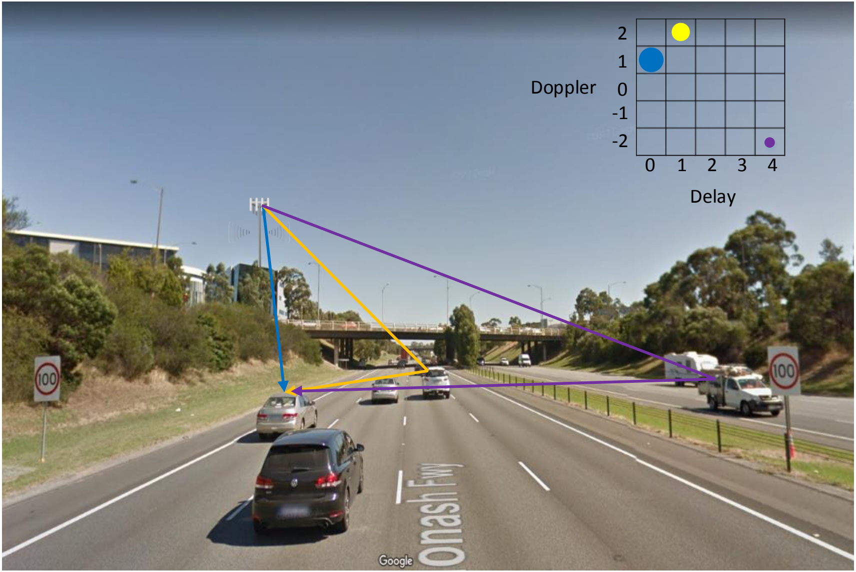

Wireless channel representation

Time-variant impulse response $g(t, \tau)$

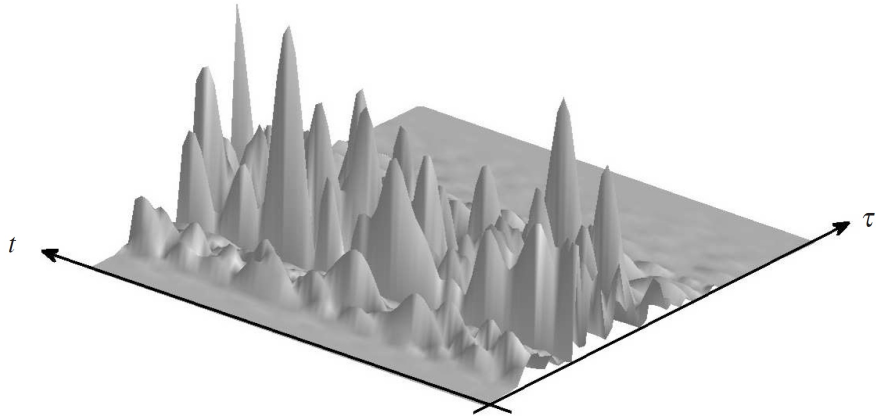

* G. Matz and F. Hlawatsch, *Chapter 1, Wireless Communications Over Rapidly Time-Varying Channels.* New York, NY, USA: Academic, 2011

Time-frequency and delay-Doppler responses

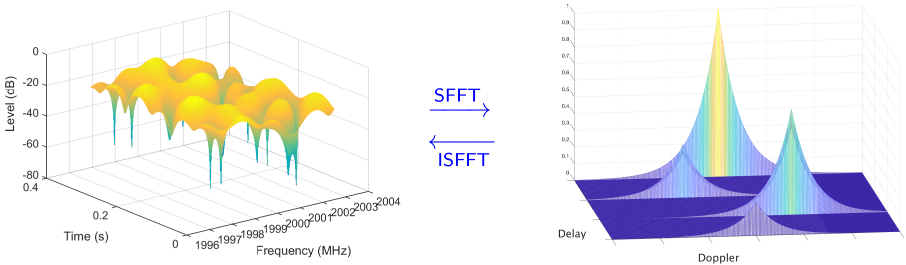

Channel in Time–frequency $H(t, f)$ and delay–Doppler $h(\tau, \nu)$

Time–Frequency and delay–Doppler grids

- Assume $\Delta f = 1/T$

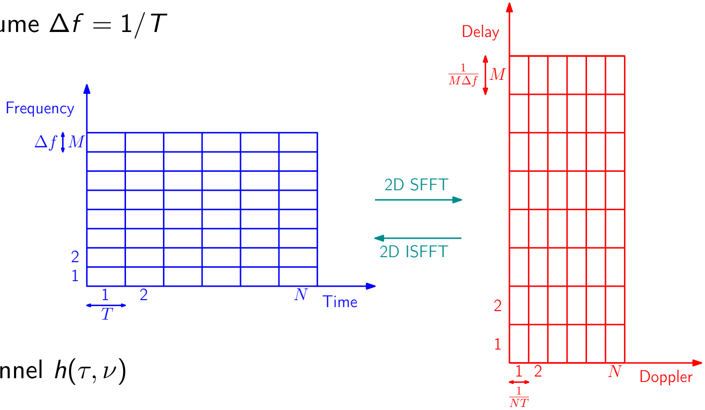

- Channel $h(\tau, \nu)$

$$h(\tau, \nu) = \sum_{i=1}^{P} h_i \delta(\tau - \tau_i)\delta(\nu - \nu_i)$$

- Assume $\tau_i = l_{\tau_i}\left(\frac{1}{M\Delta f}\right)$ and $\nu_i = k_{\nu_i}\left(\frac{1}{NT}\right)$

OTFS Parameters

Subcarrier spacing (Δf)	M	Bandwidth ($W = M\Delta f$)	Symbol duration ($T_s = 1/W$)	delay spread	$l_{\tau_{\max}}$
15 KHz	1024	**15 MHz**	0.067 μs	4.7 μs	71 ($\approx$ 7%)

Carrier frequency (f_c)	N	Latency (NMT_s $= NT$)	Doppler resolution ($1/NT$)	UE speed (v)	Doppler frequency ($f_d = f_c \frac{v}{c}$)	$k_{\nu_{\max}}$
4 GHz	128	**8.75 ms**	114 Hz	30 Kmph	111 Hz	1 ($\approx$ 1.5%)
				120 Kmph	444 Hz	4 ($\approx$ 6%)
				500 Kmph	1850 Hz	16($\approx$ 25%)

OTFS modulation

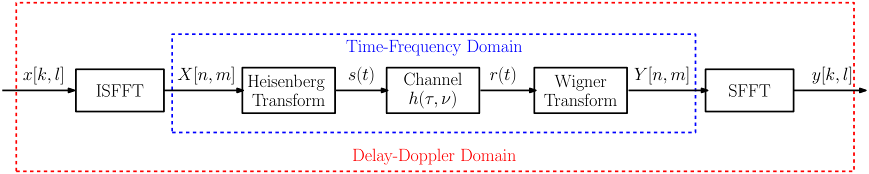

Figure: OTFS mod/demod

- Time–frequency domain is similar to an OFDM system with N symbols in a frame (Pulse-Shaped OFDM)

Time–frequency domain

- Modulator – Heisenberg transform

$$s(t) = \sum_{n=0}^{N-1} \sum_{m=0}^{M-1} X[n, m] g_{\text{tx}}(t - nT) e^{j2\pi m \Delta f (t - nT)}$$

- Simplifies to IFFT in the case of $N = 1$ and rectangular g_{tx}
- Channel

$$r(t) = \int H(t, f) S(f) e^{j2\pi f t} df$$

- Matched filter – Wigner transform

$$Y(t, f) = A_{g_{\text{rx}}, r}(t, f) \triangleq \int g^*_{\text{rx}}(t' - t) r(t') e^{-j2\pi f (t' - t)} dt'$$

$$Y[n, m] = Y(t, f)|_{t = nT, f = m\Delta f}$$

- Simplifies to FFT in the case of $N = 1$ and rectangular g_{rx}

Time–frequency domain – ideal pulses

- If g_{tx} and g_{rx} are perfectly localized in time and frequency then they satisfy the bi-orthogonality condition and

$$Y[n,m] = H[n,m]X[n,m]$$

where

$$H[n,m] = \int\int h(\tau,\nu)e^{j2\pi\nu nT}e^{-j2\pi m\Delta f\tau}d\tau d\nu$$

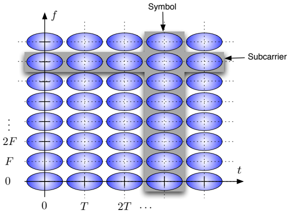

Figure: Time–frequency domain

---

* F. Hlawatsch and G. Matz, Eds., *Chapter 2, Wireless Communications Over Rapidly Time-Varying Channels.* New York, NY, USA: Academic, 2011 (PS-OFDM)

Signaling in the delay–Doppler domain

- Time–frequency input-output relation

$$Y[n, m] = H[n, m]X[n, m]$$

where

$$H[n, m] = \sum_{k} \sum_{l} h[k, l]\, e^{j2\pi\left(\frac{nk}{N} - \frac{ml}{M}\right)}$$

- ISFFT

$$X[n, m] = \frac{1}{\sqrt{NM}} \sum_{k=0}^{N-1} \sum_{l=0}^{M-1} x[k, l] e^{j2\pi\left(\frac{nk}{N} - \frac{ml}{M}\right)}$$

- SFFT

$$y[k, l] = \frac{1}{\sqrt{NM}} \sum_{n=0}^{N-1} \sum_{m=0}^{M-1} Y[n, m] e^{-j2\pi\left(\frac{nk}{N} - \frac{ml}{M}\right)}$$

Delay–Doppler domain input-output relation

- Received signal in delay–Doppler domain

$$
\begin{aligned}
y[k,l] &= \sum_{i=1}^{P} h_i x[[k-k_{\nu_i}]_N, [l-l_{\tau_i}]]_M \\
&= h[k,l] \circledast x[k,l] \qquad \text{(2D Circular Convolution)}
\end{aligned}
$$

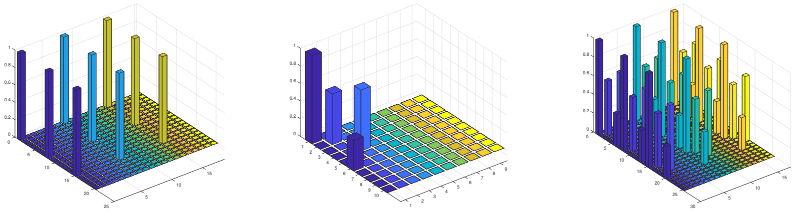

(a) Input signal, $x[k,l]$ (b) Channel, $h[k,l]$ (c) Output signal, $y[k,l]$

Figure: OTFS signals

OTFS with rectangular pulses – time–frequency domain

- Assume g_{tx} and g_{rx} to be rectangular pulses (same as OFDM) – don't follow bi-orthogonality condition

- Time–frequency input-output relation

$$Y[n, m] = H[n, m]X[n, m] + \text{ICI} + \text{ISI}$$

- ICI – loss of orthogonality in frequency domain due to Dopplers

- ISI – loss of orthogonality in time domain due to delays

(*) P. Raviteja, K. T. Phan, Y. Hong, and E. Viterbo, "Interference cancellation and iterative detection for orthogonal time frequency space modulation," *IEEE Trans. Wireless Commun.*, vol. 17, no. 10, pp. 6501-6515, Oct. 2018. Available on: https://arxiv.org/abs/1802.05242

OTFS Input-Output Relation in Matrix Form

OTFS: matrix representation

- Transmit signal at time–frequency domain: ISFFT+Heisenberg+pulse shaping on delay–Doppler

$$\mathbf{S} = \mathbf{G}_{\mathrm{tx}}\mathbf{F}_M^H \underbrace{(\mathbf{F}_M \mathbf{X} \mathbf{F}_N^H)}_{\text{ISFFT}} = \mathbf{G}_{\mathrm{tx}}\mathbf{X}\mathbf{F}_N^H$$

- In vector form:

$$\mathbf{s} = \mathrm{vec}(\mathbf{S}) = (\mathbf{F}_N^H \otimes \mathbf{G}_{\mathrm{tx}})\mathbf{x}$$

- Received signal at delay–Doppler domain: pulse shaping+Wigner+SFFT on time–frequency received signal

$$\mathbf{Y} = \mathbf{F}_M^H(\mathbf{F}_M \mathbf{G}_{\mathrm{rx}}\mathbf{R})\mathbf{F}_N = \mathbf{G}_{\mathrm{rx}}\mathbf{R}\mathbf{F}_N$$

- In vector form:

$$\mathbf{y} = (\mathbf{F}_N \otimes \mathbf{G}_{\mathrm{rx}})\mathbf{r}$$

OTFS transmitter implementation: $M = 2048$, $N = 128$

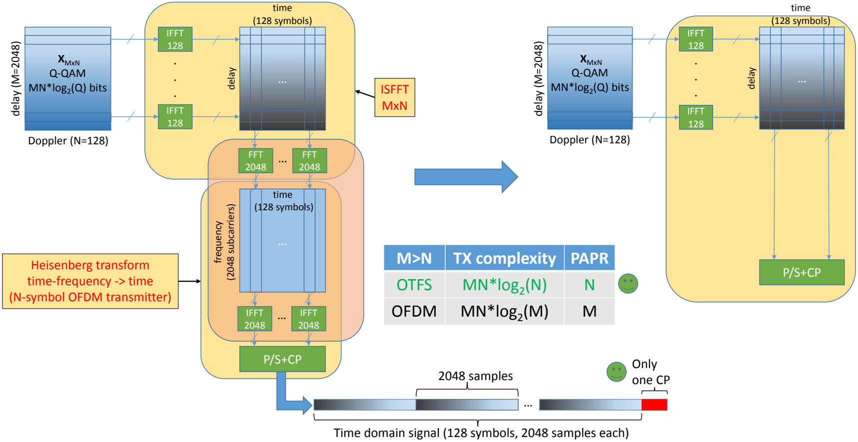

M>N	TX complexity	PAPR
OTFS	$MN*\log_2(N)$	N
OFDM	$MN*\log_2(M)$	M

- OTFS transmitter implements inverse ZAK transform (2D→1D)

OTFS receiver implementation: $M = 2048$, $N = 128$

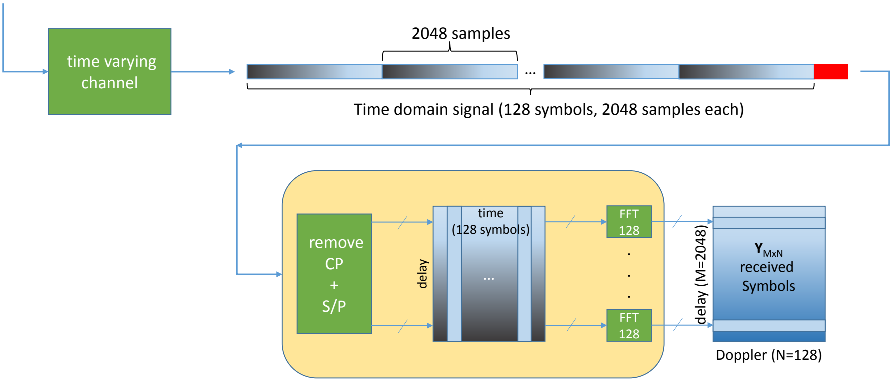

- OTFS receiver implements ZAK transform (1D→2D)

OTFS: matrix representation – channel

- Received signal in the time–frequency domain

$$r(t) = \int \int h(\tau, \nu) s(t - \tau) e^{j2\pi\nu(t-\tau)} d\tau d\nu + w(t)$$

- Channel

$$h(\tau, \nu) = \sum_{i=1}^{P} h_i \delta(\tau - \tau_i) \delta(\nu - \nu_i)$$

- Received signal in discrete form

$$r(n) = \sum_{i=1}^{P} h_i \underbrace{e^{\frac{j2\pi k_i (n-l_i)}{MN}}}_{\text{Doppler}} \underbrace{s([n - l_i]_{MN})}_{\text{Delay}} + w(n), 0 \leq n \leq MN - 1$$

OTFS: matrix representation – channel

- Received signal in vector form

$$\mathbf{r} = \mathbf{H}\mathbf{s} + \mathbf{w}$$

- $\mathbf{H}$ is an $MN \times MN$ matrix of the following form

$$\mathbf{H} = \sum_{i=1}^{P} h_i \mathbf{\Pi}^{l_i} \mathbf{\Delta}^{(k_i)},$$

where, $\mathbf{\Pi}$ is the permutation matrix (forward cyclic shift), and $\mathbf{\Delta}^{(k_i)}$ is the diagonal matrix

$$\underbrace{\mathbf{\Pi} = \begin{bmatrix} 0 & \cdots & 0 & 1 \\ 1 & \ddots & 0 & 0 \\ \vdots & \ddots & \ddots & \vdots \\ 0 & \cdots & 1 & 0 \end{bmatrix}_{MN \times MN}}_{\text{Delay (similar to OFDM)}}, \underbrace{\mathbf{\Delta}^{(k_i)} = \begin{bmatrix} e^{\frac{j2\pi k_i(0)}{MN}} & 0 & \cdots & 0 \\ 0 & e^{\frac{j2\pi k_i(1)}{MN}} & \cdots & 0 \\ \vdots & & \ddots & \vdots \\ 0 & 0 & \cdots & e^{\frac{j2\pi k_i(MN-1)}{MN}} \end{bmatrix}}_{\text{Doppler}}$$

OTFS: matrix representation – channel

- Received signal at delay–Doppler domain

$$\mathbf{y} = \left[(\mathbf{F}_N \otimes \mathbf{G}_{\rm rx})\mathbf{H}(\mathbf{F}_N^H \otimes \mathbf{G}_{\rm tx})\right]\mathbf{x} + (\mathbf{F}_N \otimes \mathbf{G}_{\rm rx})\mathbf{w}$$
$$= \mathbf{H}_{\rm eff}\mathbf{x} + \widetilde{\mathbf{w}}$$

- Effective channel for arbitrary pulses

$$\mathbf{H}_{\rm eff} = (\mathbf{I}_N \otimes \mathbf{G}_{\rm rx})(\mathbf{F}_N \otimes \mathbf{I}_M)\mathbf{H}(\mathbf{F}_N^H \otimes \mathbf{I}_M)(\mathbf{I}_N \otimes \mathbf{G}_{\rm tx})$$
$$= (\mathbf{I}_N \otimes \mathbf{G}_{\rm rx}) \underbrace{\mathbf{H}_{\rm eff}^{\rm rect}}_{\text{Channel for rectangular pulses } (\mathbf{G}_{\rm tx}=\mathbf{G}_{\rm rx}=\mathbf{I}_M)} (\mathbf{I}_N \otimes \mathbf{G}_{\rm tx})$$

- Effective channel for rectangular pulses

$$\mathbf{H}_{\rm eff}^{\rm rect} = \sum_{i=1}^{P} h_i \underbrace{\left[(\mathbf{F}_N \otimes \mathbf{I}_M)\mathbf{\Pi}^{l_i}(\mathbf{F}_N^H \otimes \mathbf{I}_M)\right]}_{\mathbf{P}^{(i)} \text{ (delay)}} \underbrace{\left[(\mathbf{F}_N \otimes \mathbf{I}_M)\mathbf{\Delta}^{(k_i)}(\mathbf{F}_N^H \otimes \mathbf{I}_M)\right]}_{\mathbf{Q}^{(i)} \text{ (Doppler)}}$$

$$= \sum_{i=1}^{P} h_i \mathbf{P}^{(i)}\mathbf{Q}^{(i)} = \sum_{i=1}^{P} h_i \mathbf{T}^{(i)}$$

OTFS: channel for rectangular pulses

- $\mathbf{T}^{(i)}$ has only one non-zero element in each row and the position and value of the non-zero element depends on the delay and Doppler values.

$$\mathbf{T}^{(i)}(p,q) = \begin{cases} e^{-j2\pi \frac{n}{N}} e^{j2\pi \frac{k_i([m-l_i]_M)}{MN}}, & \text{if } q = [m-l_i]_M + M[n-k_i]_N \text{ and } m < l_i \\ e^{j2\pi \frac{k_i([m-l_i]_M)}{MN}}, & \text{if } q = [m-l_i]_M + M[n-k_i]_N \text{ and } m \geq l_i \\ 0, & \text{otherwise.} \end{cases}$$

- Example $M = N = 2$ and $l_i = 1$ and $k_i = 1$

$$\mathbf{T}^{(i)} = \begin{bmatrix} 0 & 0 & 0 & e^{j2\pi \frac{1}{4}} \\ 0 & 0 & 1 & 0 \\ 0 & e^{-j2\pi \frac{1}{4}} & 0 & 0 \\ 1 & 0 & 0 & 0 \end{bmatrix}$$

OTFS Signal Detection

Vectorized formulation of the input-output relation

- The input-output relation in the delay–Doppler domain is a 2D convolution (with i.i.d. additive noise $w[k,l]$)

$$y[k,l] = \sum_{i=1}^{P} h_i x[[k - k_{\nu_i}]_N, [l - l_{\tau_i}]_M] + w[k,l] \quad k = 1 \dots N, l = 1 \dots M \qquad (1)$$

- Detection of information symbols $x[k,l]$ requires a deconvolution operation i.e., the solution of the linear system of NM equations

$$\mathbf{y} = \mathbf{H}\mathbf{x} + \mathbf{w} \qquad (2)$$

where $\mathbf{x}, \mathbf{y}, \mathbf{w}$ are $x[k,l], y[k,l], w[k,l]$ in vectorized form and $\mathbf{H}$ is the $NM \times NM$ coefficient matrix of (1).

- Given the sparse nature of $\mathbf{H}$ we can solve (2) by using a message passing algorithm similar to (*)

(*) P. Som, T. Datta, N. Srinidhi, A. Chockalingam, and B. S. Rajan, "Low-complexity detection in large-dimension MIMO-ISI channels using graphical models," *IEEE J. Sel. Topics in Signal Processing*, vol. 5, no. 8, pp. 1497-1511, December 2011.

Message passing based detection

- Symbol-by-symbol MAP detection

$$\begin{aligned}\widehat{x}[c] &= \arg\max_{a_j \in \mathbb{A}} \Pr\left(x[c] = a_j \,\middle|\, \mathbf{y}, \mathbf{H}\right) \\ &= \arg\max_{a_j \in \mathbb{A}} \frac{1}{Q} \Pr\left(\mathbf{y} \,\middle|\, x[c] = a_j, \mathbf{H}\right) \\ &\approx \arg\max_{a_j \in \mathbb{A}} \prod_{d \in \mathcal{J}_c} \Pr\left(y[d] \,\middle|\, x[c] = a_j, \mathbf{H}\right)\end{aligned}$$

- Received signal $y[d]$

$$y[d] = x[c]H[d,c] + \underbrace{\sum_{e \in \mathcal{I}_d, e \neq c} x[e]H[d,e] + z[d]}_{\zeta_{d,c}^{(i)} \rightarrow \text{ assumed to be Gaussian}}$$

Messages in factor graph

Algorithm 1 MP algorithm for OTFS symbol detection

Input: Received signal $\mathbf{y}$, channel matrix $\mathbf{H}$

Initialization: pmf $\mathbf{p}_{c,d}^{(0)} = 1/Q$ **repeat**

- Observation nodes send the mean and variance to variable nodes
- Variable nodes send the pmf to the observation nodes
- Update the decision

until *Stopping criteria*;

Output: The decision on transmitted symbols $\widehat{x}[c]$

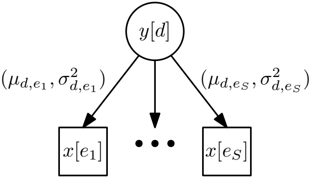

$\{e_1, e_2, \cdots, e_S\} = \mathcal{I}_d$

Observation node messages

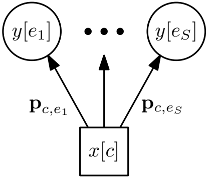

$\{e_1, e_2, \cdots, e_S\} = \mathcal{J}_c$

Variable node messages

Messages in factor graph – observation node messages

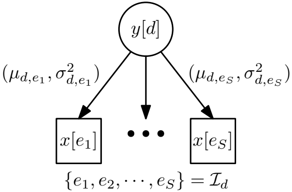

- Received signal

$$y[d] = x[c]H[d,c] + \underbrace{\sum_{e \in \mathcal{I}_d, e \neq c} x[e]H[d,e] + z[d]}_{\zeta^{(i)}_{d,c} \rightarrow \text{ assumed to be Gaussian}}$$

- Mean and Variance

$$\mu^{(i)}_{d,c} = \sum_{e \in \mathcal{I}_d, e \neq c} \sum_{j=1}^{Q} p^{(i-1)}_{e,d}(a_j) a_j H[d,e]$$

$$(\sigma^{(i)}_{d,c})^2 = \sum_{e \in \mathcal{I}_d, e \neq c} \left(\sum_{j=1}^{Q} p^{(i-1)}_{e,d}(a_j) |a_j|^2 |H[d,e]|^2 - \left| \sum_{j=1}^{Q} p^{(i-1)}_{e,d}(a_j) a_j H[d,e] \right|^2 \right) + \sigma^2$$

Messages in factor graph – variable node messages

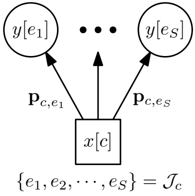

- Probability update with damping factor Δ

$$p_{c,d}^{(i)}(a_j) = \Delta \cdot \tilde{p}_{c,d}^{(i)}(a_j) + (1-\Delta) \cdot p_{c,d}^{(i-1)}(a_j), a_j \in \mathbb{A}$$

where

$$\tilde{p}_{c,d}^{(i)}(a_j) \propto \prod_{e \in \mathcal{J}_c, e \neq d} \Pr\left(y[e] \middle| x[c] = a_j, \mathbf{H}\right)$$

$$= \prod_{e \in \mathcal{J}_c, e \neq d} \frac{\xi^{(i)}(e,c,j)}{\sum_{k=1}^{Q} \xi^{(i)}(e,c,k)}$$

$$\xi^{(i)}(e,c,k) = \exp\left(\frac{-\left|y[e] - \mu_{e,c}^{(i)} - H_{e,c}a_k\right|^2}{(\sigma_{e,c}^{(i)})^2}\right)$$

Final update and stopping criterion

- Final update

$$p_c^{(i)}(a_j) = \prod_{e \in \mathcal{J}_c} \frac{\xi^{(i)}(e,c,j)}{\sum_{k=1}^{Q} \xi^{(i)}(e,c,k)}$$

$$\widehat{x}[c] = \arg\max_{a_j \in \mathbb{A}} \; p_c^{(i)}(a_j), \quad c = 1, \cdots, NM.$$

- Stopping Criterion
  - Convergence Indicator $\eta^{(i)} = 1$

$$\eta^{(i)} = \frac{1}{NM} \sum_{c=1}^{NM} \mathbb{I}\left(\max_{a_j \in \mathbb{A}} \; p_c^{(i)}(a_j) \geq 0.99 \right)$$

  - Maximum number of Iterations
- Complexity (linear) – $\mathcal{O}(n_{iter} SQ)$ per symbol which is much less even compared to a linear MMSE detector $\mathcal{O}((NM)^2)$

Simulation results – OTFS vs OFDM with ideal pulses

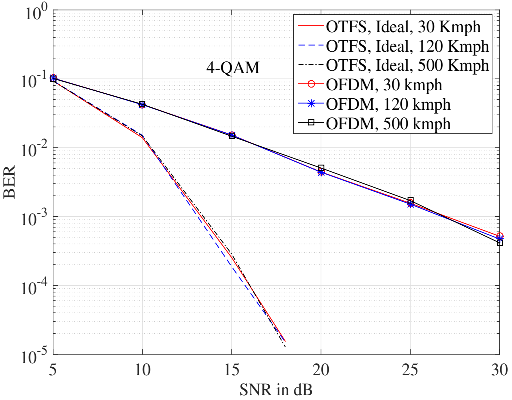

Figure: The BER performance comparison between OTFS with ideal pulses and OFDM systems at different Doppler frequencies.

Simulation results – Ideal and Rectangular pulses

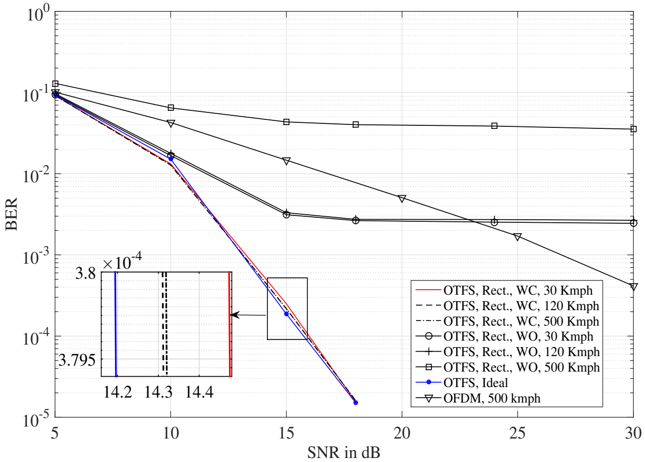

Figure: The BER performance of OTFS with rectangular and ideal pulses at different Doppler frequencies for 4-QAM.

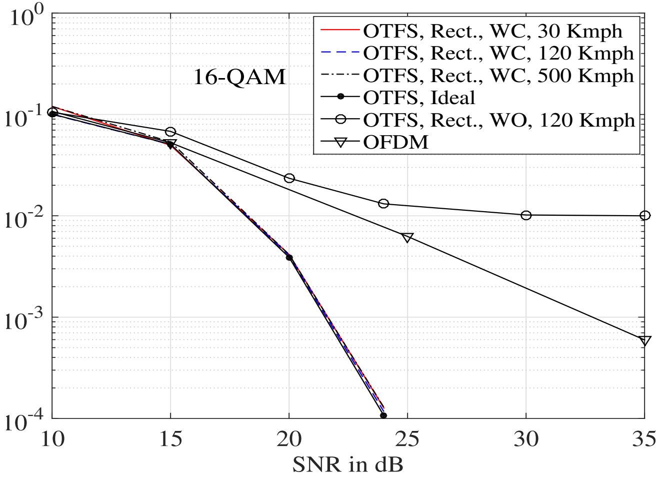

Figure: The BER performance of OTFS with rectangular and ideal pulses at different Doppler frequencies for 16-QAM.

References I

1. R. Hadani, S. Rakib, M. Tsatsanis, A. Monk, A. J. Goldsmith, A. F. Molisch, and R. Calderbank, "Orthogonal time frequency space modulation," in *Proc. IEEE WCNC*, San Francisco, CA, USA, March 2017.
2. R. Hadani, S. Rakib, S. Kons, M. Tsatsanis, A. Monk, C. Ibars, J. Delfeld, Y. Hebron, A. J. Goldsmith, A.F. Molisch, and R. Calderbank, "Orthogonal time frequency space modulation," Available online: https://arxiv.org/pdf/1808.00519.pdf.
3. R. Hadani, and A. Monk, "OTFS: A new generation of modulation addressing the challenges of 5G," *OTFS Physics White Paper*, Cohere Technologies, 7 Feb. 2018. Available online: https://arxiv.org/pdf/1802.02623.pdf.
4. R. Hadani et al., "Orthogonal Time Frequency Space (OTFS) modulation for millimeter-wave communications systems," 2017 IEEE MTT-S International Microwave Symposium (IMS), Honololu, HI, 2017, pp. 681-683.
5. A. Fish, S. Gurevich, R. Hadani, A. M. Sayeed, and O. Schwartz, "Delay-Doppler channel estimation in almost linear complexity," *IEEE Trans. Inf. Theory*, vol. 59, no. 11, pp. 7632–7644, Nov 2013.
6. A. Monk, R. Hadani, M. Tsatsanis, and S. Rakib, "OTFS - Orthogonal time frequency space: A novel modulation technique meeting 5G high mobility and massive MIMO challenges." Technical report. Available online: https://arxiv.org/ftp/arxiv/papers/1608/1608.02993.pdf.
7. R. Hadani and S. Rakib. "OTFS methods of data channel characterization and uses thereof." U.S. Patent 9 444 514 B2, Sept. 13, 2016.

References II

8. P. Raviteja, K. T. Phan, Q. Jin, Y. Hong, and E. Viterbo, "Low-complexity iterative detection for orthogonal time frequency space modulation," in *Proc. IEEE WCNC,* Barcelona, April 2018.
9. P. Raviteja, K. T. Phan, Y. Hong, and E. Viterbo, "Interference cancellation and iterative detection for orthogonal time frequency space modulation," *IEEE Trans. Wireless Commun.*, vol. 17, no. 10, pp. 6501-6515, Oct. 2018.
10. P. Raviteja, K. T. Phan, Y. Hong, and E. Viterbo, "Embedded delay-Doppler channel estimation for orthogonal time frequency space modulation," in Proc. IEEE VTC2018-fall, Chicago, USA, August 2018.
11. P. Raviteja, K. T. Phan, and Y. Hong, "Embedded pilot-aided channel estimation for OTFS in delay-Doppler channels," accepted in *IEEE Transactions on Vehicular Technology*.
12. P. Raviteja, Y. Hong, E. Viterbo, and E. Biglieri, "Practical pulse-shaping waveforms for reduced-cyclic-prefix OTFS," *IEEE Trans. Veh. Technol.*, vol. 68, no. 1, pp. 957-961, Jan. 2019.
13. P. Raviteja, Y. Hong, and E. Viterbo, "OTFS performance on static multipath channels," *IEEE Wireless Commun. Lett.*, Jan. 2019, doi: 10.1109/LWC.2018.2890643.
14. P. Raviteja, K.T. Phan, Y. Hong, and E. Viterbo, "Orthogonal time frequency space (OTFS) modulation based radar system," accepted in *Radar Conference*, Boston, USA, April 2019.

References III

15. Li Li, H. Wei, Y. Huang, Y. Yao, W. Ling, G. Chen, P. Li, and Y. Cai, "A simple two-stage equalizer with simplified orthogonal time frequency space modulation over rapidly time-varying channels," available online: https://arxiv.org/abs/1709.02505.
16. T. Zemen, M. Hofer, and D. Loeschenbrand, "Low-complexity equalization for orthogonal time and frequency signaling (OTFS)," available online: https://arxiv.org/pdf/1710.09916.pdf.
17. T. Zemen, M. Hofer, D. Loeschenbrand, and C. Pacher, "Iterative detection for orthogonal precoding in doubly selective channels," available online: https://arxiv.org/pdf/1710.09912.pdf.
18. K. R. Murali and A. Chockalingam, "On OTFS modulation for high-Doppler fading channels," in *Proc. ITA'2018,* San Diego, Feb. 2018.
19. M. K. Ramachandran and A. Chockalingam, "MIMO-OTFS in high-Doppler fading channels: Signal detection and channel estimation," available online: https://arxiv.org/abs/1805.02209.
20. A. Farhang, A. RezazadehReyhani, L. E. Doyle, and B. Farhang-Boroujeny, "Low complexity modem structure for OFDM-based orthogonal time frequency space modulation," in *IEEE Wireless Communications Letters,* vol. 7, no. 3, pp. 344-347, June 2018.
21. A. RezazadehReyhani, A. Farhang, M. Ji, R. R. Chen, and B. Farhang-Boroujeny, "Analysis of discrete-time MIMO OFDM-based orthogonal time frequency space modulation," in *Proc. 2018 IEEE International Conference on Communications (ICC),* Kansas City, MO, USA, pp. 1-6, 2018.

Thank you!!